Electronic Supplementary Material (ESI) for ChemComm.

Supporting Information for:

A Co(TAML)-Based Artificial Metalloenzyme for Asymmetric Radical-Type Oxygen Atom Transfer Catalysis

Eva J. Meeus,[1] Nico V. Igareta,[2] Iori Morita,[2] Thomas R. Ward,[2,*] Bas de Bruin,[1,*] Joost N. H. Reek[1,*]

[1]Homogeneous, Supramolecular and Bio-Inspired Catalysis Group, Van 't Hoff Institute for Molecular Sciences (HIMS), University of Amsterdam, Science Park 904, 1098 XH Amsterdam, The Netherlands. [*]b.debruin@uva.nl, [*]j.n.h.reek@uva.nl

[2]Forschungsgruppe Ward, Department of Chemistry, University of Basel, Mattenstrasse 22, CH-4002 Basel, Switzerland. [*]thomas.ward@unibas.ch

Table of contents

General considerations

Materials and methods

All reagents were of commercial grade (Acros Organics, Sigma-Aldrich, Alfa Aesar, Fluorochem, Merck, Fisher) and used without further purification, unless noted otherwise. Dry MeOH and DMF were purchased from Sigma Aldrich or Acros Organics and used without further purification. Dry THF was distilled from sodium benzophenone ketyl. Streptavidin (Sav) mutants were produced, purified and characterized as previously described.[1] All catalytic reactions were performed in 2 mL glass vials under aerobic conditions at room temperature (±27 °C) with magnetic stirring, unless noted otherwise.

Instrumentation

^{1}H-NMR spectra were recorded on a Bruker DRX 300, Bruker DRX 500, or Bruker Avance Neo spectrometer at 25 °C and the reported ppm (parts per million) values are relative to SiMe4. Data was processed and visualized using MestReNova, version 14.1.0. High-resolution mass spectra (HRMS) were measured on a Bruker maXis4G QTOF ESI mass spectrometer using H_2O:HCO_2H 0.1% or MeCN:HCO_2H 0.1% (for positive mode) or MeOH (for negative mode) as the solvent. GC-HRMS measurements were performed on a AccuTOF GC v 4g, JMS-T100GCV mass spectrometer (JEOL, Japan). Typical measurement conditions are as follows: positive-ion mode; filament ionizing voltage 70V. FI probe equipped with FI emitter, Carbotec (Germany), FI 10 µm. Flashing current 40 mA on every spectra of 20 ms. Counter electrode -10kV, Ion source 37V. UV-Vis spectra were recorded on a Shimadzu UV-2000 spectrophotometer in a 10 mm quartz cuvette from 190 to 800 nm. ITC measurements were performed on a Microcal VP-ITC apparatus. Catalytic runs were analyzed by a GC-FID equipped with a CP-Chirasil-Dex CB column (25m 0.25mm 0.25 µm) using He as carrier gas. The water used in the catalytic reactions was purified by a Milli-Q Advantage system. A Water Prep LC 4000 System equipped with a Dr. Maisch, Reprospher, 100 C18-DE column (40 × 150 mm, 5 µm, 100Å) was used to purify compound **4**. A Biotage isolera one system equipped with a Biotage SNAP Ultra C18 column was used to purify **biot^{C4}-1'**.

Section 1: Cofactor synthesis

2-methyl-2-phthalimidopropanoic acid,[2, 3] phthalimidoisobutyrylchloride,[2, 3] compound **1**-**3**[4] and norbotinamine[5, 6, 7] were synthesized following previously reported procedures.

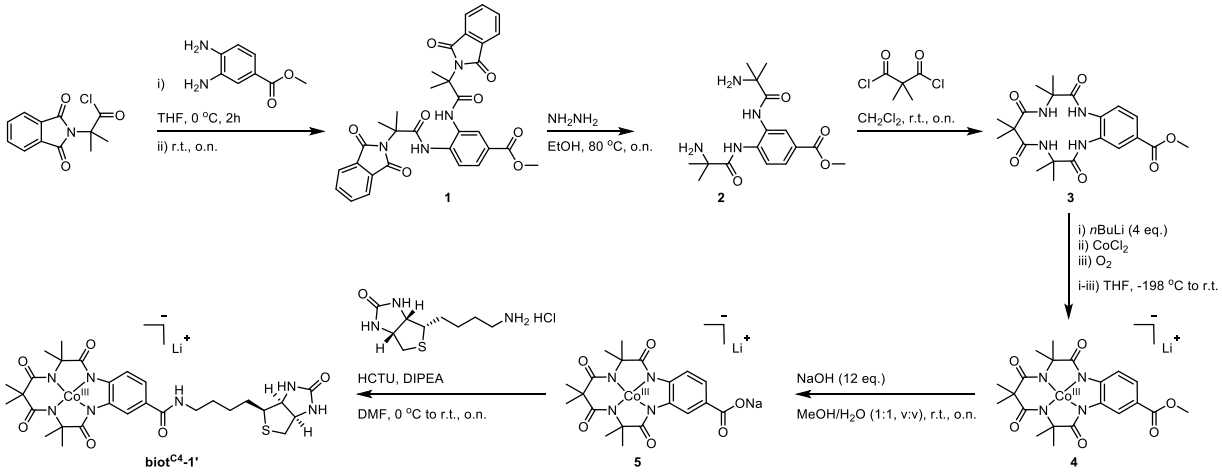

Scheme S1 Synthetic route pursued for the synthesis of **biot^{C4}-1'**.

*Compound **4***

The synthesis of compound **4** was based on a previously reported procedure.[2] Compound **3** (284.3 mg, 0.66 mmol, 1.0 eq.) was dissolved in THF (35 mL, dry and degassed) under nitrogen in a 100 mL flame-dried Schlenk. The solution was frozen at -198 °C and *n*BuLi (2.5 M in hexanes, 1 mL, 2.48 mmol, 4.0 eq.) was added dropwise, upon which the solid started to melt. Just before the solid finished thawing, $CoCl_2$ (anhydrous, 106.8 mg, 0.806 mmol, 1.3 eq) was added in one portion under nitrogen flow. The solution was stirred at r.t. for 30 min and became grey-green, after which the solution was bubbled with air for 90 min. to form a purple suspension. The suspension was transferred onto a silica column with THF and the purple band eluted with acetone. The purple solution was evaporated under reduced pressure. The product was suspended in DCM (200 mL) and washed with diethyl ether (200 mL) after collection via filtration. The purple crystalline powder was dried under vacuum and purified by reverse phase chromatography with a Dr. Maisch, Reprospher, 100 C18-DE column. Compound **4** was purified by the following procedure: H_2O : ACN = 97 : 3, flow rate 20 mL/min, method: 0 min – 0% B; 2.5 min – 10% B; 30 min – 90% B; 32 min – 100%; 36 min – 100%. Purified compound **4** was obtained after evaporating all solvent under reduced pressure. Isolated yield: 32.4 mg, 0.066 mmol, 10%.

^{1}H NMR (400 MHz, CD_3CN) δ 6.96 (s, 3H), 4.73 (d, 12H), 3.74 (s, 6H), -3.88 (s, 1H), -7.03 (s, 1H), -15.27 (s, 1H).
HRMS (ESI negative mode) $C_{21}H_{24}CoN_4O_6$ $[M]^-$ calcd: 487.1033 *m/z*, found: 487.1038 *m/z*.
UV/Vis (CH_3CN) λ_{max} (nm) (ε) = 199.5 (30756), 252 (18733), 510.5 (636).
Evans' method: MeOD with H_2O as an internal standard, c = 0.02003 M, Δ*v* = 184.75 Hz, μ_{eff} = 3.316 μ_B (S = 1), χ_d = -0.00020638 emu mol^{-1}.

biot^{C4}-1'

The synthesis of **biot^{C4}-1'** was based on a previously reported procedure via compound **5**.[4] Compound **4** (32.4 mg, 0.066 mmol, 1 eq.) was dissolved MeOH (2.5 mL, dry) in a 25 mL round-bottom. A solution of NaOH (33.6 mg, 0.787 mmol, 12 eq.) in Milli-Q water (2 mL) was added and the purple reaction mixture was stirred at 40 °C overnight. The reaction mixture was evaporated to dryness to yield the crude purple compound **5**, which was used in the next step without further purification. The reaction progress was monitored by ESI-MS.

Compound **5** was transferred to a 10 mL Schlenk and a nitrogen atmosphere was established. After addition of norbiotinamine·HCl (16.6 mg, 0.066 mmol, 1 eq.), DMF (3 mL, dry) was added to dissolve all reagents and the reaction mixture was cooled to 0 °C. A pre-cooled solution of HCTU (38.22 mg, 0.092 mmol, 1.4 eq.) in DMF (2 mL, dry) was added dropwise to the reaction mixture, followed by the addition of DIPEA (32 µL, 0.1848 mmol, 2.8 eq.). The reaction mixture was stirred at r.t. overnight. To reach full conversion, another batch of HCTU (19.11 mg, 0.047 mmol, 0.7 eq.) and DIPEA (16 µL, 0.092 mmol, 1.4 eq.) were added after cooling the reaction mixture to 0 °C, which was then allowed to warm up to r.t. and stirred for another 1.5 h. The reaction progress was monitored by ESI-MS. The solvent was evaporated under reduced pressure to yield a purple solid, which was redissolved in MeOH (2.5 mL, dry). The product was precipitated by addition of diethyl ether (20 mL), which was decanted after centrifugation, washed with diethyl ether (40 mL) and left to dry at r.t. The crude product was redissolved in Milli-Q water (2 mL) and all insoluble material was removed by centrifugation. The product was finally purified by reverse phase chromatography using a Biotage SNAP Ultra C18 column. **biot^{C4}-1'** was eluted at 55% MeOH using a gradient H_2O:MeOH. Purified **biot^{C4}-1'** was obtained after evaporating all solvent under reduced pressure and dried under vacuum. Isolated yield: 10.5 mg, 0.015 mmol, 23%.

HRMS (ESI negative mode) $C_{29}H_{37}CoN_7O_6S$ $[M]^-$ calcd: 670.1864 *m/z*; found: 670.1877 *m/z*.
Crystal structures of **biot^{C4}-1'** · Sav WT and **biot^{C4}-1'** · Sav S112Y; see Section 2.

Section 2: Characterization of the CoTAML-based artificial metalloenzyme

ITC measurements

The biotin binding affinity was determined using a Microcal VP-ITC apparatus following a previously described procedure.[8] **biot^{C4}-1'** (250 µM) in 50 mM potassium phosphate buffer containing 100 mM sodium chloride was titrated with 5 µL injections of Sav-WT solutions (40 µM, 50 mM potassium phosphate buffer, 100 mM sodium chloride). The reference cell contained the same buffer as the protein and cofactor solutions. Measurements were performed at 25 °C. The **biot^{C4}-1'** binding affinity (K_a), enthalpy (H), and binding stoichiometry (N) were calculated using ITC data analysis origin software (MicroCal) and the results are presented in Figure S1. Based on both measurements a K_d of 1.84*10^{-8} M was derived given that $K_d = \frac{1}{K_a}$.

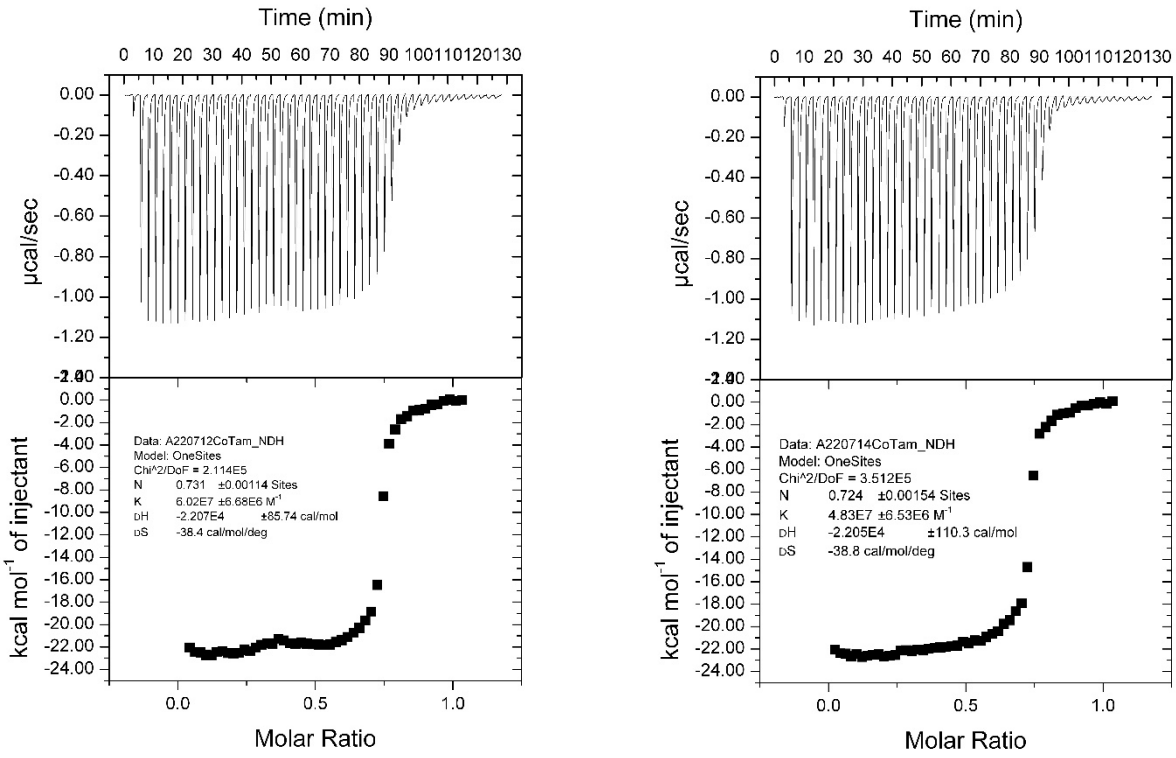

Figure S1: ITC measurements performed in duplicate.

HABA displacement titration

Following the previously described protocols,[4, 9, 10, 11] a solution of Sav WT (2.4 mL, initial concentration 8.0 µM tetrameric Sav WT in 20 mM phosphate buffer pH 7) was loaded in a UV-Vis cuvette. To this solution, a large excess of 2-(4-hydroxyphenylazo)benzoic (HABA, 300 µL 9.6 mM in 20 mM phosphate buffer pH 7, 150 equiv versus Sav) was added to ensure full saturation of the active sites. **biot^{C4}-1'** (0.96 mM in Milli-Q water) was added to the HABA/Sav solution in 0.25 equiv aliquots (5 µL per step, up to 5 equiv) relative to the tetrameric protein. The UV-Vis spectrum was recorded 2 min after each addition, and the decrease of the absorbance at λ_{max} = 506 nm was plotted against the equivalents of **biot^{C4}-1'** added (Figure S2). The decrease ceases after the addition of around 4 equiv of **biot^{C4}-1'**. This result indicates a Sav_{tet} WT : **biot^{C4}-1'** ratio of 1 : 4, which is in line with previous reports.[4] Because of the background absorbance of the cofactor at 506 nm, we did not fit the HABA titration results to derive the K_d.

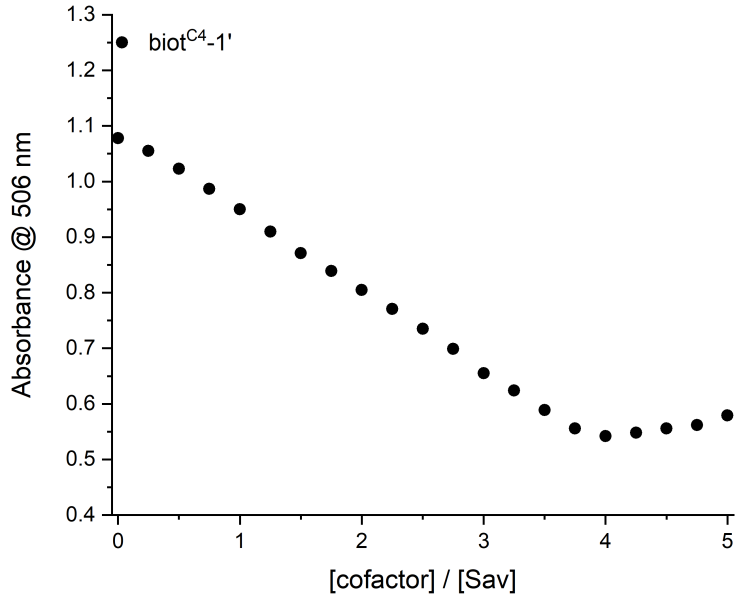

Figure S2: HABA displacement titration assay by **biot^{C4}-1'** in Sav WT (black dots).

X-ray crystallography

For sitting drop vapor diffusion, the Sav isoforms Sav WT and Sav S112Y (2.0 µL, 20 mg/mL, in Milli-Q water) were mixed with the precipitation buffer (2.0 µL, 2 M $(NH_4)_2SO_4$, 0.1 M Na-Acetate, pH 4). The drop was equilibrated against a reservoir of precipitation buffer (100 µL). Crystals of apo-Sav grew within 3 days. For soaking, apo-crystals were transferred into sitting-drop depressions containing precipitation buffer (4.5 µL adjusted at pH 6) and cofactor solution (0.5 µL, 10 mM **biot^{C4}-1'** in Milli-Q water). As no influence on catalyst activity was observed by changing **biot^{C4}-1'** to Sav and the homotetrameric structure of Sav during initial screenings (*vide infra*), a full saturation of binding sites was aimed for. Moreover, the homotetrameric structure of streptavidin challenges the formation and characterization of a homogeneous 2:1 Sav : cofactor ratio, given the non-cooperative nature of the biotin-binding events. After soaking (for 20 h, 20 °C) the crystals were directly flash-frozen in liquid nitrogen.

Protein crystal diffraction data were collected at 100 K at the Swiss Light Source beam line PXI at a wavelength of 1.0 Å. Crystal indexing, integration and scaling were carried out with the program XDS[12] and reflections were merged with the program aimless[13] of the CCP4i2 Suite[14] (see Table X and X for processing statistics). REFMAC5[15, 16] was used for structure refinement. For structure modelling, water picking and electron density visualization the software COOT[17, 18] was used. Figures were prepared with PyMOL (the PyMOL Molecular Graphics System, Version 2.3.0, Schrödinger, LLC). The structure was solved by molecular replacement using the program PHASER MR[19] and the Sav structure (PDB code: 3PK2, devoid of the Ir-cofactor and water molecules).

One homotetramer of the Sav proteins was obtained per asymmetric unit. Amino acid residues 1-12, 135-197 presumably due to disorder. Residual electron density in the F_o-F_c map was observed in the biotin binding pocket and in the biotin vestibule, as well as anomalous dispersion density. Modeling of cofactor **biot^{C4}-1'** into the electron density projected the cobalt in the position of the anomalous density peak. The occupancy of the cobalt atom in **biot^{C4}-1'** is 100% for Sav WT and Sav S112Y.

Table S1: Data processing and crystal structure refinement statistics.

Sav	Sav WT	Sav S112Y
Cofactor	**biot^{C4}-1'** (PDB: VJC)	**biot^{C4}-1'** (PDB: VJC)
PDB Code	8CRP	8CRN
Data Processing Statistics		
Resolution Range (Å)	45.91-2.00 (2.05-2.00)	45.92-2.00 (2.05-2.00)
Cell Parameters		
- a, b, c (Å)	192.50, 57.70, 57.70	192.51, 57.61, 57.61
- α, β, γ (°)	90.00, 107.44, 90.00	90.00, 107.41, 90.00
Space group	C121	C121
Unique reflections	276705 (20880)	256680 (19460)
Rmerge (%)	10.4 (148.4)	10.1 (92.5)
Multiplicity	6.9 (7.0)	6.4 (6.5)
Mean I/Sig(I)	10.3 (1.4)	10.7 (2.3)
Completeness (%)	98.2 (98.4)	98.6 (99.3)
CC (1/2)	0.998 (0.577)	0.998 (0.718)
Structure Refinement Statistics		
R_{work}/R_{free}	0.20/0.21	0.19/0.21
Average B-factors (Å)	43.0	39.0

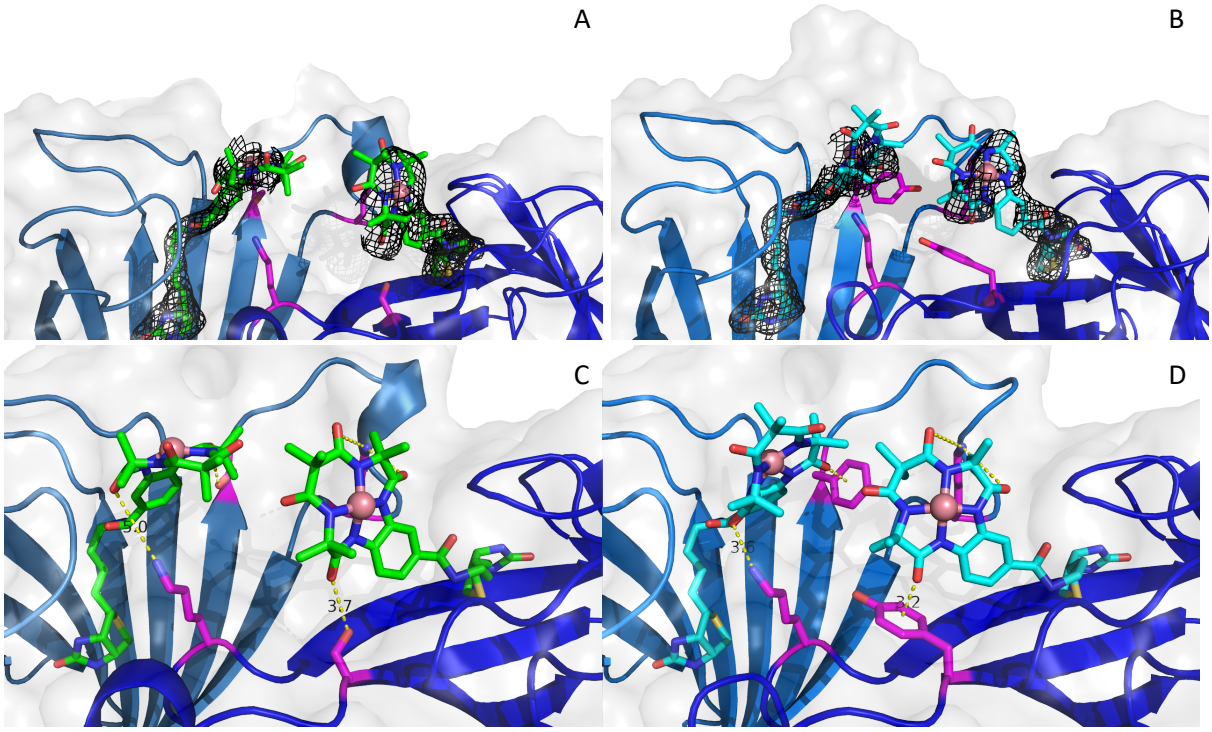

Figure S3: Structural analysis of the artificial metalloenzymes (A) **biot^{C4}-1'** · Sav WT, and (B) **biot^{C4}-1'** · Sav S112Y. Close-up view of the X-ray crystal structure of (C) **biot^{C4}-1'** · Sav WT (PDB: 8CRP), and (D) **biot^{C4}-1'** · Sav S112Y (PDB: 8CRN). The **biot^{C4}-1'** cofactor is displayed as green (A/C) or cyan (B/D) sticks (atoms are color-coded; nitrogen: blue, oxygen: red, carbon: green or cyan, chloride: green, and sulfur: yellow), and the cobalt center as a pink sphere. The protein is displayed as a cartoon- and transparent surface-accessible model. The monomers are color-coded in different shades of blue. The residues S112 and K121 are displayed as purple sticks (atoms are color-coded; nitrogen: blue, oxygen: red, and carbon: purple). The $2F_o$-F_c difference map is displayed as dark grey mesh (1σ) (A/B). The occupancy of the cobalt center was set to 100%. The closest contacts between the side-chains of the amino acids at position S112 and the **biot^{C4}-1'** cofactor are highlighted as a yellow dotted line (C = 3.7 Å; D = 3.2 Å, respectively). The distances between K121 and the **biot^{C4}-1'** cofactor are also shown as a yellow dotted line (C = 4.0-5.0 Å; D = 3.6-4.8 Å, respectively).

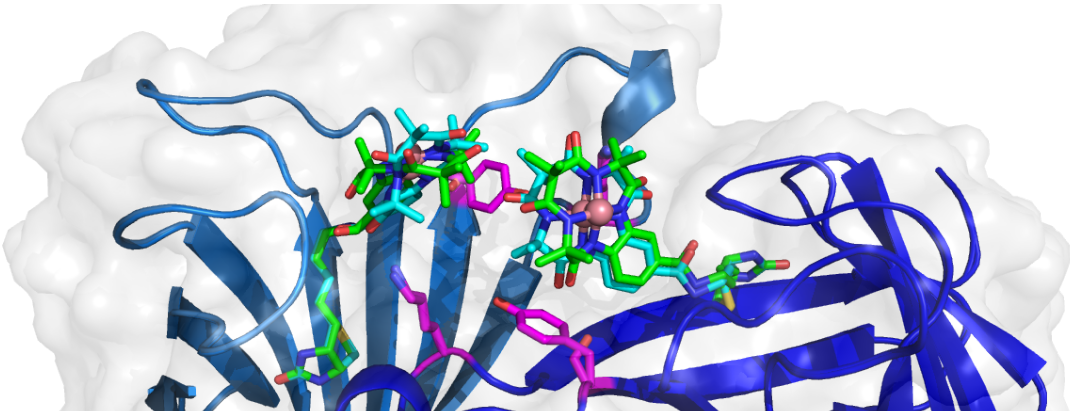

Figure S4: Superposition of both crystal structures (PDB: 8CRP and 8CRN). The **biot^{C4}-1'** cofactor of Sav WT is displayed as green sticks and of Sav S112Y in cyan sticks.

Section 3: Catalysis experiments

Catalytic epoxidation

The general procedure, based on a previously reported procedure,[4] was adapted after optimization of the reaction conditions: *O*-source/oxidant, pH, Buffer, **biot^{C4}-1'** : Sav ratio, and catalyst loading (mol %). Note that no activity was observed with oxidants (e.g., NaO_3Cl, H_2O_2, $KHSO_4$, NaOCl), and similar activity was observed with **biot^{C4}-1'** : Sav_{tet} ratio's 1:1, 2:1, 4:1. Side product formation was observed at pH 7 and below. Despite considerable efforts, we were thus far not able to perform nitrene transfer catalysis with the Co(TAML)-based artificial metalloenzyme.

General procedure for catalytic experiments

In a typical experiment, **biot^{C4}-1'** (0.021 µmol, 0.5 mol %) was dissolved in Milli-Q water (100 µL) and a stock solution of the desired Sav mutant (100 µL, 0.2 M in potassium phosphate buffer (KPB) pH 8). Then, the solution was left to incubate for 20 min after which the substrate (21 µmol) and PhIO (4.2 µmol) were added. The vial was sealed with a cap, and the reaction mixture was stirred (500 rpm) for 2 h. 1,3,5-tritertbutylbenzene (100 µL of a stock solution in $CDCl_3$) was added as an external standard. After addition of another 600 µL of $CDCl_3$, the reaction mixture was extracted and filtered (syringe filter, PTFE, 0.45 mm) to remove unreacted iminoiodinane. The $CDCl_3$ layer was analyzed by ^{1}H NMR spectroscopy after which it was dried over $MgSO_4$, filtered through a short cotton plug and subjected to analysis with GC-FID. The results of the catalytic experiments are summarized in Table S2.

Characterization of the reaction product

α-methylstyrene oxide was prepared from α-methylstyrene and PhIO according to the above-mentioned procedure with **biot^{C4}-1'** · Sav. A crude ^{1}H NMR spectrum for the formation of α-methylstyrene oxide is depicted in Figure S6 and is in accordance with literature.[20] The resonance for 1,3,5-tritertbutylbenzene at δ = 1.33 ppm and the characteristic signals for α-methylstyrene oxide at δ = 2.80 and 2.97 ppm were used to calculate the total turnover number (TTON). The enantiomeric excess (ee) of α-methylstyrene oxide was determined by GC analysis [Chirasil-Dex CB, injector temp. = 80 °C, detector temp. = 225 °C , column temp. = 80 °C (isothermic)]. The absolute configurations of the two enantiomers was assigned by comparing the retention times with those reported in the literature,[21] i.e., t = 15.9 ((*R*)-α-methylstyrene oxide), t = 16.9 ((*S*)-α-methylstyrene oxide). A crude GC chromatogram for (*rac*)-α-methylstyrene oxide, and the formation of ee 28% (*S*)-α-methylstyrene oxide and ee 45% (*R*)-α-methylstyrene oxide are depicted in Figure S7-Figure S9, respectively.

Catalysis experiment in the presence of the radical trap DMPO

A 2 mL glass vial containing 0.021 µmol (0.5 mol %) **biot^{C4}-1'** was charged with Milli-Q water (75 µL) and a stock solution of Sav WT (100 µL, 0.2 M in potassium phosphate buffer (KPB) pH 8) to dissolve the cofactor. Then, the solution was left to incubate for 20 min. While incubating, a fresh stock solution of DMPO (0.84 M) in degassed Milli-Q water was prepared. After incubation, 25 µL of the DMPO stock solution was added to the reaction mixture, after which the substrate (21 µmol) and PhIO (4.2 µmol) were added. The vial was closed with a cap and the reaction mixture was stirred (500 rpm) for 2 h. 1,3,5-tritertbutylbenzene (100 µL of a stock solution in $CDCl_3$) was added as an internal standard. After addition of another 600 µL of $CDCl_3$, the reaction mixture was extracted and filtered (syringe filter, PTFE, 0.45 mm) to remove unreacted iminoiodinane. The $CDCl_3$ layer was analyzed by ^{1}H NMR spectroscopy. The result of this catalytic experiment is reported in Table S2, entry 3.

Control experiment in the presence of biotin

Two separate stock solutions of biotin and Sav S112M (0.84 mM in potassium phosphate buffer (KPB) pH 8) were prepared. From both stock solutions, 100 µL was added to a 2 mL glass vial and the solution was left to incubate for 20 min. A 2 mL glass vial containing 0.021 µmol (0.5 mol %) cofactor was charged with Milli-Q water (100 µL) and the biotin · Sav S112M stock solution (100 µL). Then, the solution was left to incubate for another 20 min after which the substrate (21 µmol) and PhIO (4.2 µmol) were added. The vial was sealed with a cap, and the reaction mixture was stirred (500 rpm) for 2 h. 1,3,5-tritertbutylbenzene (100 µL of a stock solution in $CDCl_3$) was added as an internal standard. After addition of another 600 µL of $CDCl_3$, the reaction mixture was extracted and filtered (syringe filter, PTFE, 0.45 mm) to remove unreacted iminoiodinane. The $CDCl_3$ layer was analyzed by ^1H NMR spectroscopy, after which it was dried over $MgSO_4$, filtered through a short cotton plug, and subjected to analysis with GC-FID. The result of this control experiment is reported in Table S2, entry 9.

Control experiment in $H_2{}^{18}O$

As an additional control experiment, the reaction was performed in $H_2{}^{18}O$, following the above-described '*General procedure for catalytic experiments*.' After extraction in $CDCl_3$, product formation was confirmed by ^1H NMR spectroscopy and the reaction mixture was further analyzed by GC-FI measurements. The result is depicted in Figure S5.

Subjecting **biot^{C4}-1'** · Sav S112M to PhIO and α-methylstyrene in $H_2{}^{18}O$ afforded styrene oxide with and without incorporation of ^{18}O as supported by the GC-FI measurements. Given that the presence of PhIO and **biot^{C4}-1'** · Sav S112M are crucial for the reaction to occur (Table S2, entry 4 and 5), the formed oxyl radical intermediate likely undergoes exchange with water, as suggested by the incorporation of ^{18}O in the epoxide product.

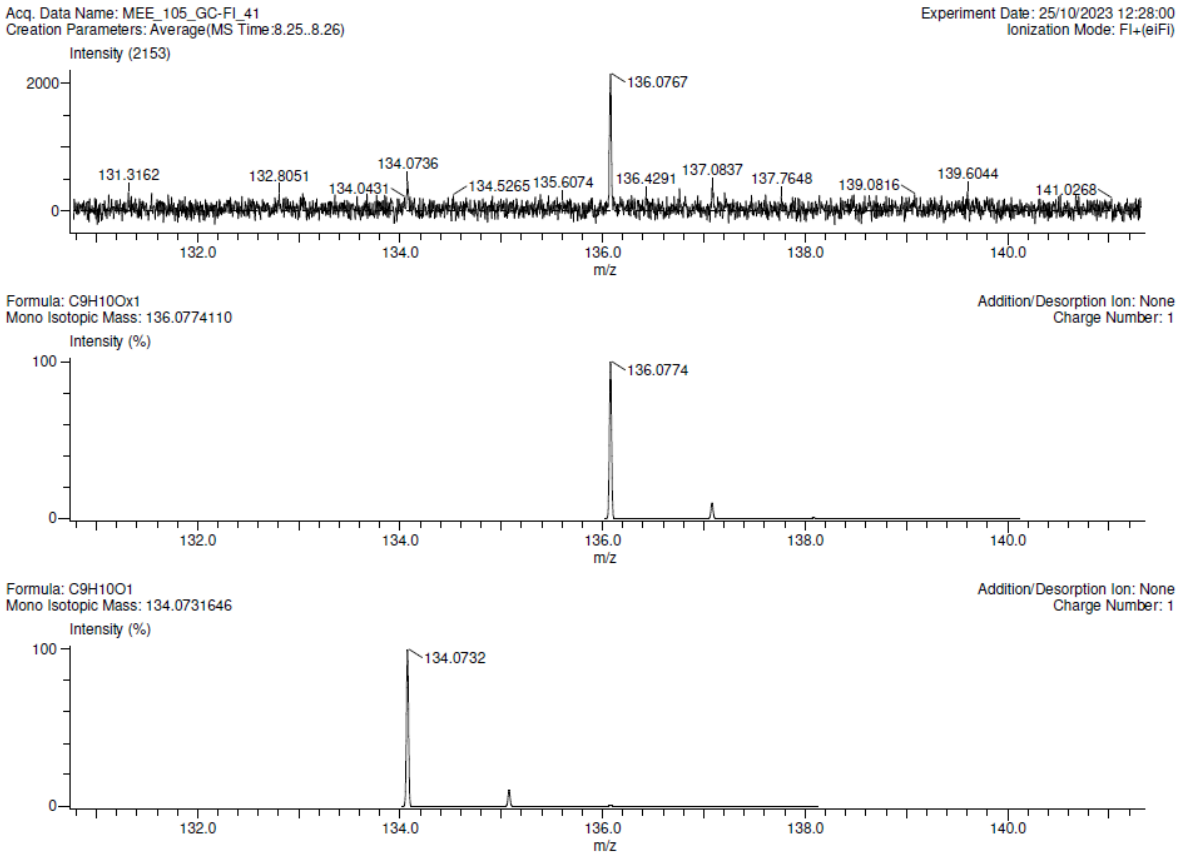

Figure S5: HRMS-FI spectrum of α-methylstyrene oxide (top) with ^{18}O incorporation (measured: 136.0767 *m/z*, calculated: 136.0774 = middle) and without ^{18}O incorporation (measured: 134.0736 *m/z*, calculated: 134.0732 *m/z*) after performance of the standard reaction in $H_2{}^{18}O$(98%).

Table S2: Numerical summary of the results of the catalytic reactions with **biot^{C4}-1'** using α-methylstyrene and PhIO as the substrate and *O*-source, respectively. The total turnover number corresponds to the sum of cycles (turnovers) that the catalyst undergoes to yield the product over the course of 2 h, and are derived from the yields determined with ^{1}H NMR spectroscopy. The enantiomeric excess was determined by GC-FID analysis.

Entry[a]	**Sav**	**Yield (%)**	**TTON**	**ee**[b]
1[c]	No Sav	0	n.d.	n.d.
2[c]	WT	0	n.d.	n.d.
3	WT *+ DMPO*	traces	n.d.	n.d.
4[c]	S112M	0	n.d.	n.d.
5[d]	S112M	0	n.d.	n.d.
5[e]	No Sav	16	33	1
6[e]	WT	16	32	11
7	S112A	28	56	13
8[e]	S112M	22	44	32
9	S112M *+ biotin*	18	37	6
10[e]	S112T	30	62	-11
11[e]	S112R	23	47	26
12[e]	S112G	32	61	0
13[e]	S112Y	21	42	-22
14	S112Q	16	34	7
15	S112H	15	31	-4
16	S112K	21	42	10
17	S112E	11	22	1
18	S112C	11	23	6
19	S112F	20	42	-4
20	S112L	21	41	-16
21	K121M	25	52	3
22	K121W	19	38	0
23	K121S	16	33	0
24	K121F	20	41	5
25	K121R	27	56	10
26	K121A	10	20	4
27	K121I	11	23	-8
28	K121P	15	32	11
29	K121H	9	18	0
30[e]	K121D	11	22	-8
31	K121C	10	20	5
32	S112A/K121L	19	39	12
33[e]	S112Y/K121R	23	46	-28
34	S112Y/K121E	19	38	2
35	S112Y/K121S	16	32	-19
36	S112R/K121A	22	46	17
37	S112M/K121E	17	34	-4
38[e]	S112M/K121R	19	38	45

[a] Reaction conditions: 0.105 mM **biot^{C4}-1'**, 0.21 mM Sav, 0.1 M KPB pH 8, 104.5 mM α-methylstyrene, 21 mM PhIO, 2h, 27 °C, aerobic atmosphere. [b] Positive values indicate the ee of (*R*)-α-methylstyrene, negative values the ee of (*S*)-α-methylstyrene. [c] Experiment performed in the absence of cofactor. [d] Experiment performed in the absence of PhIO. [e] Experiment was performed at least in duplicate.

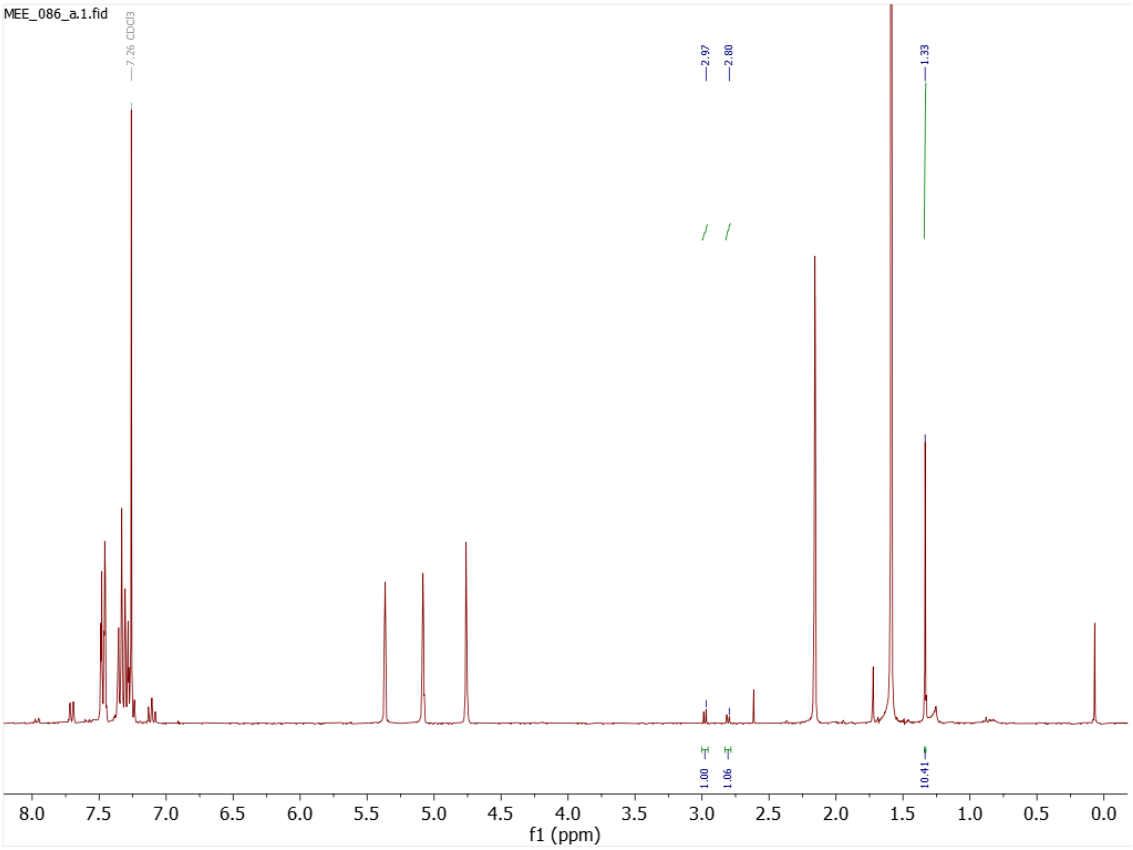

Figure S6: Crude ^{1}H NMR spectrum of α-methylstyrene oxide in $CDCl_3$ wherein **biot^{C4}-1'** · Sav WT (0.5 mol %) was used as the catalyst, with 0.3 µmol 1,3,5-tritertbutylbenzene as internal standard.

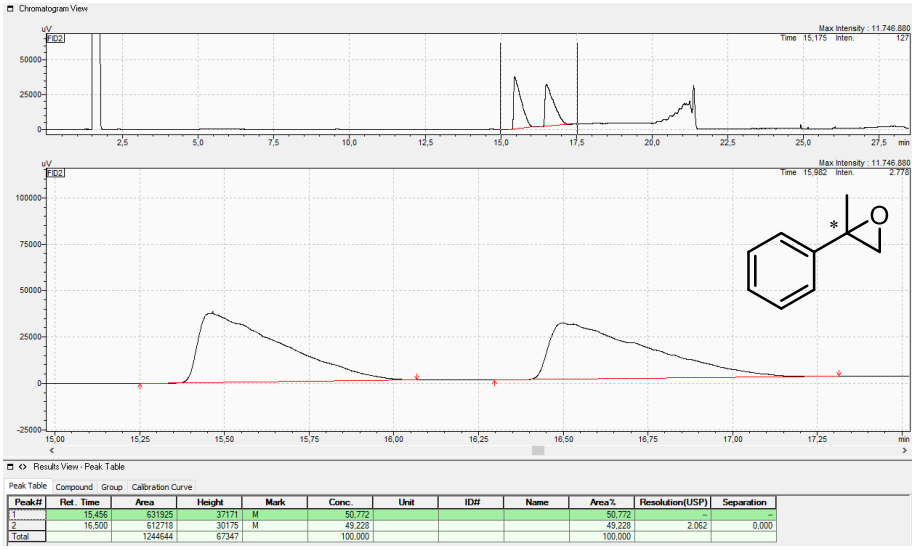

Figure S7: GC-FID chromatogram of purified (*rac*)-α-methylstyrene oxide.

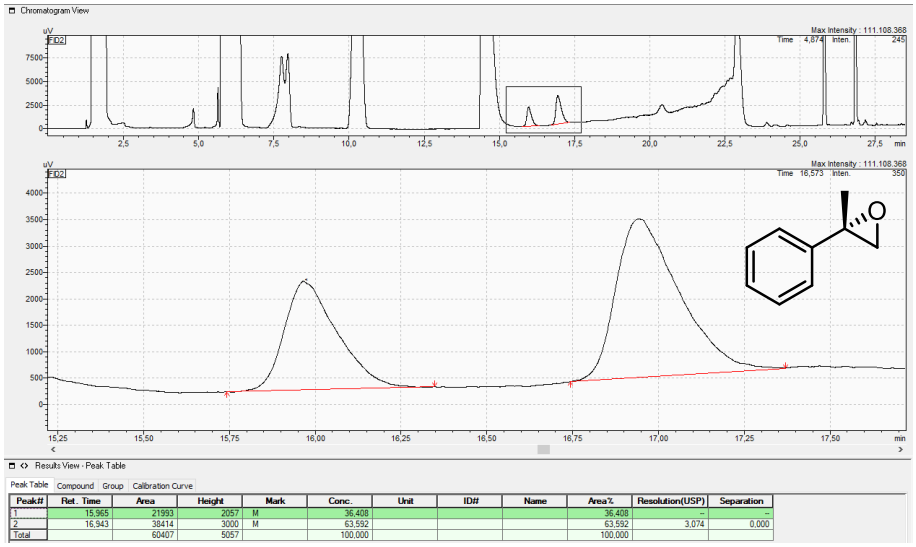

Figure S8: Crude GC-FID chromatogram of ee 28% (*S*)-α-methylstyrene oxide wherein **biot^{C4}-1'** · Sav S112Y/K121R (0.5 mol %) was used as the catalyst.

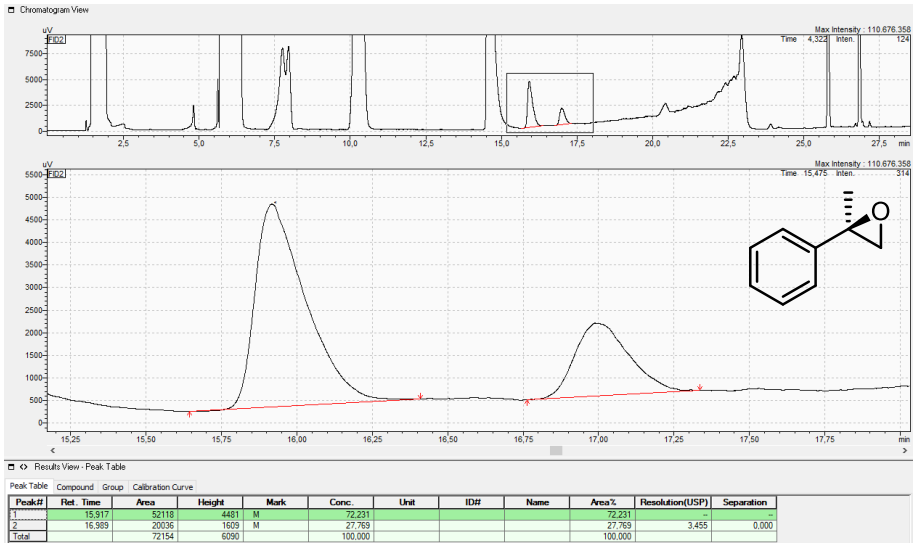

Figure S9: Crude GC-FID chromatogram of ee 45% (*R*)-α-methylstyrene oxide wherein **biot^{C4}-1'** · Sav S112M/K121R (0.5 mol %) was used as the catalyst.

Experimental spectra

*Compound **4***

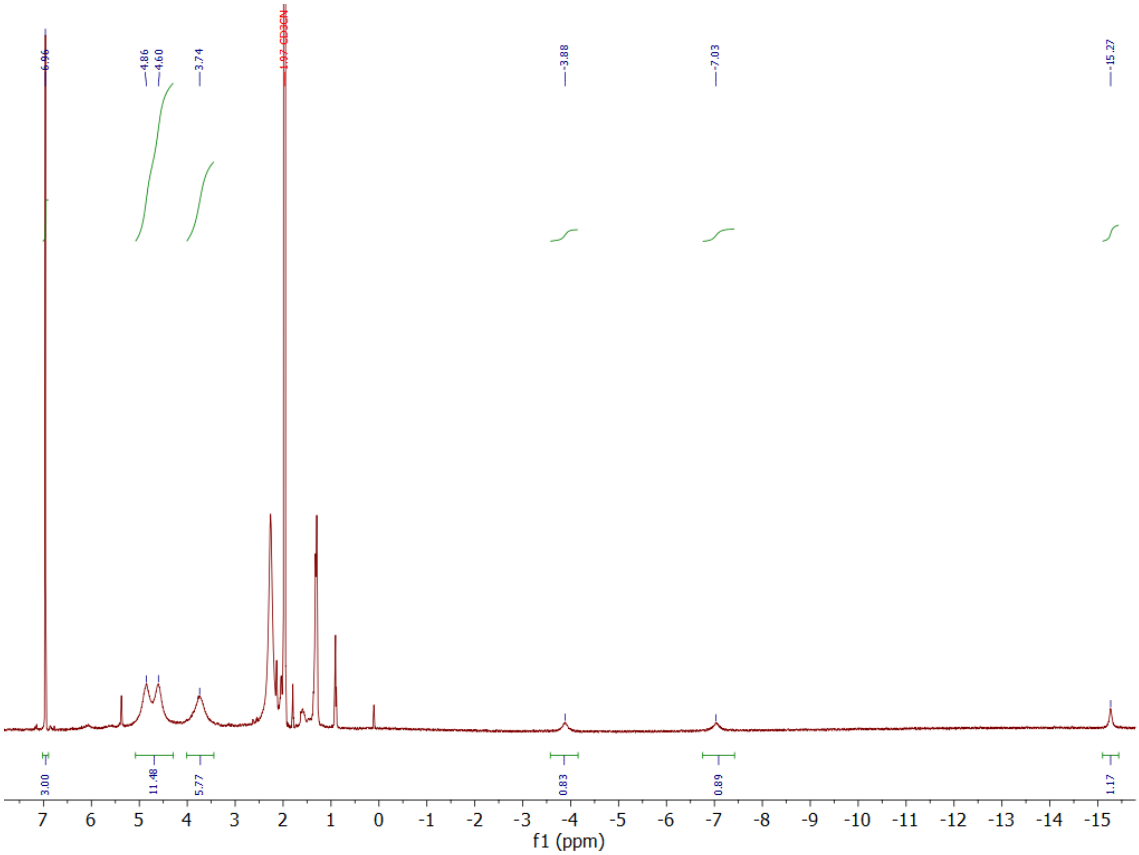

Figure S10: ^{1}H NMR of compound **4** (400 MHz, CD_3CN, 298 K).

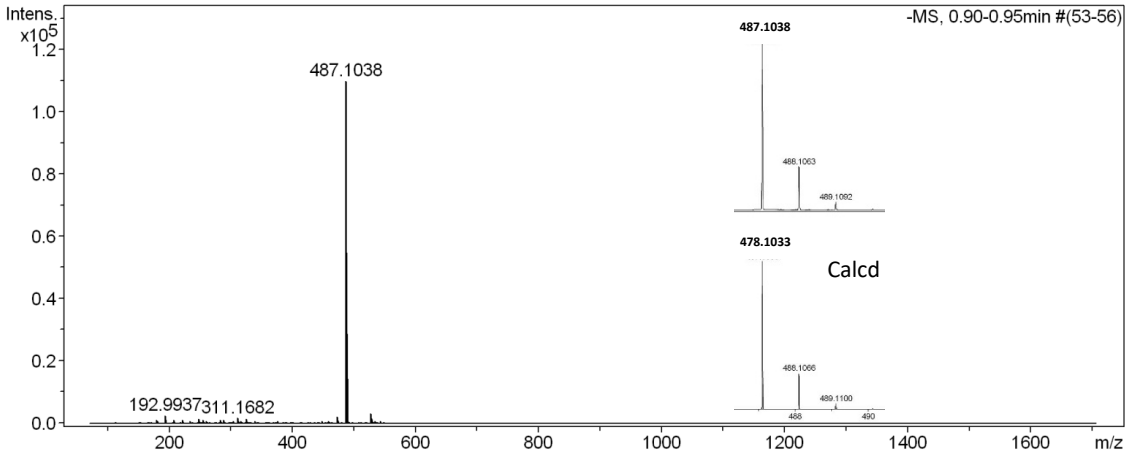

Figure S11: ESI-HRMS spectrum of compound **4** (negative mode).

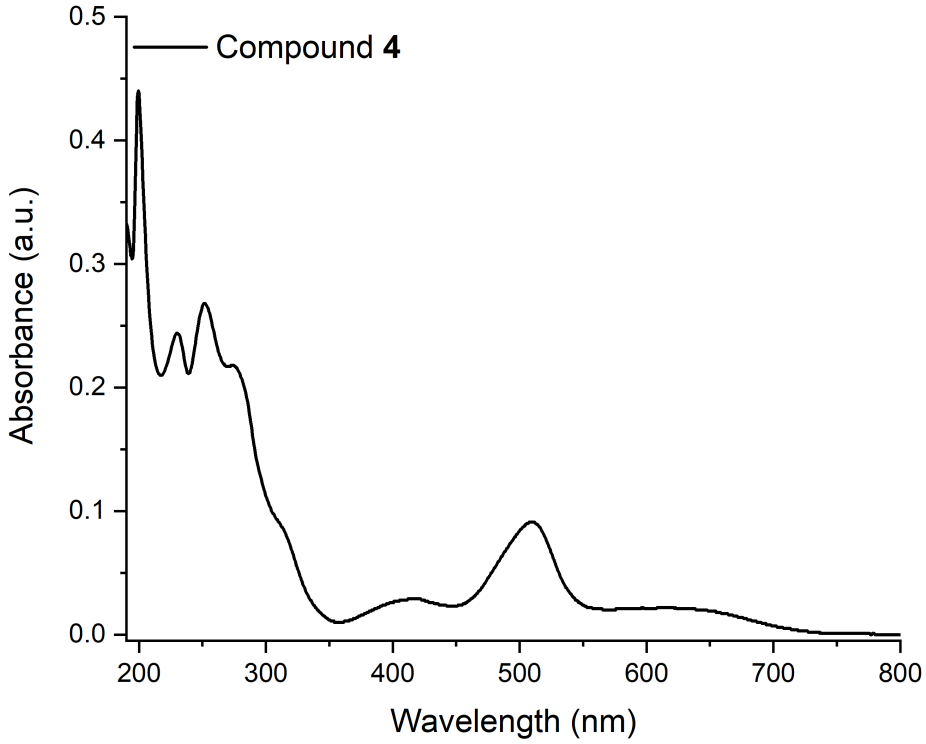

Figure S12: UV-Vis spectrum of compound **4** in MeOH

biot^{C4}-1'

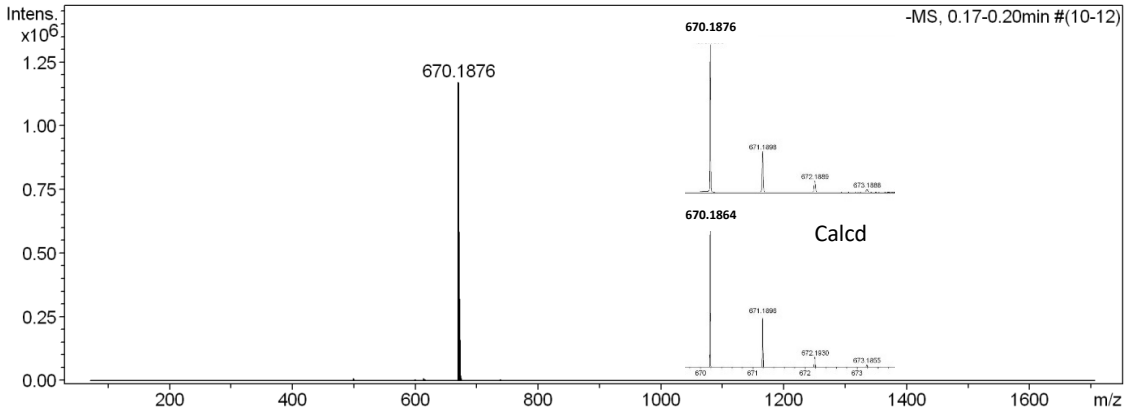

Figure S13: ESI-HRMS spectrum of **biot^{C4}-1'** (negative mode).

Acknowledgements

Financial support from the research priority area Sustainable Chemistry of the University of Amsterdam and the Holland Research School of Molecular Chemistry PhD Mobility Program is gratefully acknowledged. Hua Yong, Manjistha Mukherjee and Elinor Morris (Uni Basel) are kindly acknowledged for experimental support. Ed Zuidinga (UvA) and Felix de Zwart (UvA) for help with HRMS measurements and helpful suggestions, respectively. All other members of the Ward lab and HomKat group, past and present, are gratefully thanked for fruitful discussions and support.

References

[1] H. Mallin, M. Hestericová, R. Reuter, T. R. Ward, *Nat. Protoc.* **2016**, *11*, 835–852.
[2] N. P. van Leest, M. A. Tepaske, J.-P. H. Oudsen, B. Venderbosch, N. R. Rietdijk, M. A. Siegler, M. Tromp, J. I. van der Vlugt, B. de Bruin, *J. Am. Chem. Soc.* **2019**, *142*, 552–563.
[3] P. Ramidi, S. Z. Sullivan, Y. Gartia, P. Munshi, W. O. Griffin, J. A. Darsey, A. Biswas, A. U. Shaikh, A. Ghosh, *Ind. Eng. Chem. Res.* **2011**, *50*, 7800–7807.
[4] J. Serrano-Plana, C. Rumo, J. G. Rebelein, R. L. Peterson, M. Barnet, T. R. Ward, *J. Am. Chem. Soc.* **2020**, *142*, 10617–10623.
[5] T. P. Soares da Costa, W. Tieu, M. Y. Yap, O. Zvarec, J. M. Bell, J. D. Turnidge, J. C. Wallace, G. W. Booker, M. C. J. Wilce, A. D. Abell, S. W. Polyak, *ACS Med. Chem. Lett.* **2012**, *3*, 509–514.
[6] W. Szalecki, *Bioconjugate Chem.* **1996**, *7*, 271–273.
[7] R. C. Brewster, G. C. Gavins, B. Günthardt, S. Farr, K. M. Webb, P. Voigt, A. N. Hulme, *Chem. Commun.* **2016**, *52*, 12230–12232.
[8] V. Chu, P. S. Stayton, S. Freitag, I. Le Trong, R. E. Stenkamp, *Protein Sci.* **1998**, *7*, 848–859.
[9] H. J. Lin, J. F. Kirsch, *Anal. Biochem.* **1977**, *81*, 442–446.
[10] G. Kada, K. Kaiser, H. Falk, H. J. Gruber, *Biochim. Biophys. Acta* **1999**, *1427*, 44–48.
[11] M. Skander, N. Humbert, J. Collot, J. Gradinaru, G. Klein, A. Loosli, J. Sauser, A. Zocchi, F. Gilardoni, T. R. Ward, *J. Am. Chem. Soc.* **2004**, *126*, 14411–14418.
[12] W. Kabsch, *Xds. Acta Crystallogr., Sect. D: Biol. Crystallogr.* **2010**, *66 (Pt 2)*, 125–32.
[13] P. R. Evans, G. N. Murshudov, *Acta Crystallogr., Sect. D: Biol. Crystallogr.* **2013**, *69 (Pt 7)*, 1204–14.
[14] L. Potterton, J. Agirre, C. Ballard, K. Cowtan, E. Dodson, P. R. Evans, H. T. Jenkins, R. Keegan, E. Krissinel, K. Stevenson, A. Lebedev, S. J. McNicholas, R. A. Nicholls, M. Noble, N. S. Pannu, C. Roth, G. Sheldrick, P. Skubak, J. Turkenburg, V. Uski, F. von Delft, D. Waterman, K. Wilson, M. Winn, M. Wojdyr, *Acta Cryst. D* **2018**, *74 (Pt 2)*, 68–84.
[15] O. Kovalevskiy, R. A. Nicholls, F. Long, A. Carlon, G. N. Murshudov, *Acta Crystallogr., Sect. D: Biol. Crystallogr.* **2018**, *74 (Pt 3)*, 215–227.
[16] G. N. Murshudov, P. Skubak, A. A. Lebedev, N. S. Pannu, R. A. Steiner, R. A. Nicholls, M. D. Winn, F. Long, A. A. Vagin, *Acta Crystallogr. Sect. D.* **2011**, *67 (Pt 4)*, 355–67.
[17] P. Emsley, B. Lohkamp, W. G. Scott, K. Cowtan, *Acta Crystallogr., Sect. D: Biol. Crystallogr.* **2010**, *66 (Pt 4)*, 486–501.
[18] P.Emsley, K. Cowtan, *Acta Crystallogr., Sect. D: Biol. Crystallogr.* **2004**, *60 (Pt 12, Pt 1)*, 2126–32.
[19] A. J. McCoy, R. W. Grosse-Kunstleve, P. D. Adams, M. D. Winn, L. C. Storoni, R. J. Read, *J. Appl. Crystallogr.* **2007**, *40 (Pt 4)*, 658–674.
[20] C. Molinaro, A.-A. Guilbault, B. Kosjek, *Org. Lett.* **2010**, *12*, 3772–3775.
[21] T. Sone, A. Yamaguchi, S. Matsunaga, M. Shibasaki, *J. Am. Chem. Soc.* **2008**, *130*, 10078–10079.